Geological Quarterly, 2026, 70, 15
DOI: https://doi.org/10.7306/gq.1860

Lithological trend analysis using well logging and geological data for improved reservoir rock identification – the Krosno Beds (Oligocene–Miocene), the Outer Polish Carpathians

Paulina I. KRAKOWSKA-MADEJSKA[1, *], Krzysztof STARZEC[2], Sebastian WASZKIEWICZ[1], Jadwiga A. JARZYNA[1], Edyta PUSKARCZYK[1] and Anita LIS-ŚLEDZIONA[3]

1 AGH University of Krakow, Faculty of Geology, Geophysics and Environmental Protection, Department of Geophysics, al. A. Mickiewicza 30, 30-059 Kraków, Poland; ORCID: 0000-0002-8261-4350 [P.I.K.], 0000-0002-0887-770X [S.W.], 0000-0001-5277-0507 [E.P.], 0000-0002-1803-8643 [J.A.J.]

2 AGH University of Krakow, Faculty of Geology, Geophysics and Environmental Protection, Department of General Geology and Geotourism, al. A. Mickiewicza 30, 30-059 Kraków, Poland; ORCID: 0000-0001-6538-5296

3 Oil and Gas Institute – National Research Institute, ul. Lubicz 25A, 31-503 Kraków, Poland; ORCID: 0000-0003-3067-3014

Krakowska-Madejska, P.I., Starzec, K., Waszkiewicz, S., Jarzyna, J.A., Puskarczyk, E., Lis-Śledziona, A., 2026. Lithological trend analysis using well logging and geological data for improved reservoir rock identification – the Krosno Beds (Oligocene–Miocene), the Outer Polish Carpathians. Geological Quarterly, **70**, 15; https://doi.org/10.7306/gq.1860

Associate Editor: Piotr Krzywiec

The Integrated Predictive Error Filter Analysis (INPEFA) technique was applied to investigate lithological variations with the aim of enhancing the identification of reservoir intervals within a sandstone-shale succession. The study utilized geological and well logging data from three boreholes penetrating the Krosno Beds in the Silesian Unit (Jurassic–Neogene) of the Outer Carpathians. Available well logs were reinterpreted to delineate petrophysical lithofacies based on shale content. Effective porosity (PHI) and estimated permeability values (K) were employed to calculate the Flow Zone Index (FZI) and classify Rock Types. Macroscopic core and cuttings descriptions, supplemented by field geological observations, facilitated the identification of geological lithofacies. These geological and petrophysical lithofacies, along with Rock Types, were correlated with INPEFA curves derived from well log parameters including gamma ray (GR), spontaneous potential (SP), bulk density (RHOB), and acoustic transit time (DT), as well as reinterpreted effective porosity (PHI) and shale volume (VCL). Facies classification within the sandstone-shale profiles of the Krosno Beds was refined by analysing INPEFA trends and inflection points. The integration of multiple analytical approaches based on various scale data, i.e. well logs, results of macroscopic analysis of cutting samples and cores together with information from geological field studies enabled a more precise delineation of intervals showing favourable reservoir properties within the stratigraphic columns. The study presented shows that information from various sources and on various scales, combined for a single purpose – lithofacies identification – results in a more accurate lithological recognition, which also affects understanding of reservoir properties. The trends obtained from the Cyclolog program made it possible to generalize very detailed and, by necessity, fragmented information from well logging and, at the same time, to responsibly incorporate independent, multi-scale data from core, cutting sample and field information.

Key words: lithofacies, reservoir properties, INPEFA trend analyses, well logging, geological data, petrophysical lithofacies.

INTRODUCTION

The assessment of the oil and gas or water-bearing reservoir potential of rock is based on specific geological and petrophysical characteristics. The key parameters are porosity and permeability, etermined on the basis of laboratory tests of drill cores and interpretation of well logging data. However, initial information about the possible reservoir capacity of the formations analysed is obtained from geological knowledge about the area based on specialist literature, field geological studies and macroscopic analyses of cores, cuttings, and surface rock samples (e.g., Wells, 1967; Hallenburg, 1998; Asquith and Krygowski, 2004; Catuneanu, 2006; Tiab and Djebbar, 2015; Dziadzio et al., 2021; Crain's Petrophysical Handbook, 2025).

The facies model, constructed on the basis of geological reconnaissance, including mineralogical, petrographic, and geochemical analyses, as well as the results of well logging measurements and interpretation, is very helpful in assessing the

* Corresponding author, e-mail: krakow@agh.edu.pl

Received: October 17, 2025; accepted: May 18, 2026; first published online: June 29, 2026

reservoir capacity of rocks. For years, various data processing techniques, the most up-to-date at the time, have been used to create the product in the form of the information about the reservoir rock potential. The simplest use of well logging data to identify lithofacies is based on cross-plots constructed using logs, e.g., P-wave transit interval time (DT) from acoustic logs vs. neutron porosity (NPHI) from neutron logs or bulk density (RHOB) vs. photoelectric absorption index (PE) from spectral gamma-gamma logs (e.g., Schlumberger, 1999; Serra, 2008). A similar approach can be taken with laboratory test results for porosity and permeability by constructing a Flow Zone Index (FZI) based on this data. However, the success of the traditional approach requires very careful preparation of well logs and a significant number of laboratory tests, which is not always possible. Modern analyses performed on samples cut from cores, polished sections or drill cuttings are a projection of the latest capabilities of equipment on rock material. However, their point-like nature is always the dominant feature, overshadowing the latest technical achievements. In the case of well logging, which provides a large amount of regularly and continuously sampled data, the use of statistical methods provides new information, regardless of the methodologies used (Das et al., 2024). The combination of various techniques is always an effective way to enrich information about facies and petrophysical properties (Bała et al., 2012; Ma, 2019; Wang et al., 2025).

The goal of the present research is to enhance the assessment of reservoir capacity in rocks by integrating geological information with well logging data. This involves using both traditional and modern analytical techniques, including INPEFA spectral trend analysis, lithofacies identification and Flow Zone Index calculations to more accurately characterize the petrophysical properties and lithological variability of the Krosno Beds in the Outer Carpathians. The study demonstrates that combining diverse data sources and methods improves precision in identifying reservoir formations.

The most important aspect of the work presented is the combination of geological information and well logging data, taking into account their specific characteristics and capabilities. INPEFA (Spectral Trend Attribute Analysis) analyses for the preliminary identification of lithological changes were included based on the results of well logs and their geological interpretation (i.e. studies of the shapes of SP, GR and other well logging curves as a function of the sedimentary environment; Galloway, 1989; Catuneanu, 2006; Shouket and Jarzyna, 2014). At the same time, lithofacies were identified based on the results of quantitative interpretation of well logging and macroscopic analyses of cores, and of cuttings that were related to rocks exposed at the surface. Rock types were also determined based on FZI coefficients, which define the ability of reservoir media flow. INPEFA change graphs as a function of depth facilitated the identification of characteristic points on well logs associated with changes in lithology and/or sedimentary conditions and facies. The research material consisted of a sandstone-shale succession of the Krosno Beds in the eastern part of the Outer Carpathians, in which the sandstone intervals constitute one of the reservoir rocks of hydrocarbon fields identified and exploited in this area. It was shown that the inclusion of an additional tool allowed for a more accurate identification of the reservoir capacity of the rocks studied.

GEOLOGICAL SETTING

The Silesian Unit stretches from the Moravian Beskids to the Bieszczady Mountains (Książkiewicz, 1977; Fig. 1). The Unit is represented by sedimentary rocks ranging in age from the Upper Jurassic (Tithonian) to the Paleogene (Oligocene). The formations of the Silesian Unit in the Polish Outer Carpathians comprise a wide range of strata deposited in the central part of the Carpathian Basin. The average sedimentary thickness of this Unit is 2,500–3,000 m. In the central part of this Unit, there is a structure known as the Central Carpathian Depression (Tołwiński, 1933). The Silesian Unit within the Central Carpathian Depression is mainly composed of facies-diverse formations of the Menilite-Krosno series (Oligocene–Lower Miocene). The formations of this Unit are divided into two facies zones: the Lesko zone in the north-east and the Otryt (Bieszczady) zone in the south-west (Żytko, 1968 *fide* Malata and Zimnal, 2013). These zones differ from each other first of all in terms of the lithostratigraphic profile of the Krosno Beds, particularly as regards the position of the thick-bedded sandstone members that dominate in both zones, secondly in terms of the age at which the sedimentation of the Krosno Beds began (earlier in the south), and above all in terms of transport directions and petrographic composition of the main sandstone succession (Ślączka, 1980; Malata et al., 2006; Malata and Zimnal, 2013). Namely, the Otryt Sandstone Member is composed of medium- to coarse-grained sandstones that are characterized by low mineralogical maturity, consisting of quartz, micas and feldspars and relatively high amounts of metamorphic rock clasts. Grains are usually poorly rounded, which also indicates the low textural maturity of these sandstones (Ślączka and Unrug, 1972; Godlewski et al., 2016). By comparison, the Lesko Sandstone Member is built of mostly fine- to medium-grained sandstones, rich in quartz, feldspars and muscovite and with some sedimentary and metamorphic rock clasts (Malata et al., 2006). Well-rounded grains in these sandstones document their high textural maturity (Godlewski et al., 2016).

The different mineral compositions, textural maturities and transport directions are inferred to result from different source areas for these two facies (Ślączka et al., 1975; Wendorff, 1986). The boreholes P-1, ST-1, and TN-1 analysed are located in the southern Otryt facies zone, which consists of the following lithostratigraphic units: Menilite Beds, Transitional Beds, Lower Krosno Beds (divided into three members: the Zatwarnica Member, the Otryt Sandstone Member, and the Supra-Otryt Member; Table 1).

Geological cross-sections illustrating the structure of the area have been prepared based on the surface data (Fig. 1B), from which the predicted profiles of the boreholes studied can be interpreted:

- the ST-1 borehole is located on the Otryt Sandstone Member, but close to the boundary with the Zatwarnica Member. It can be concluded that the upper part of the stratigraphic column consists mainly of the thick-bedded Otryt Sandstone Member and, at a depth of ~300 m, the borehole reaches the underlying Zatwarnica Member (folded thin- and medium-bedded sandstones and shales), while in the bottommost part, the borehole probably crosses the base of the Zatwarnica thrust fold and enters again the Otryt Sandstone Member that forms the southern limb of the next, more northern fold (Fig. 2A).
- the P-1 borehole is located within the Otryt Sandstone Member. Due to the slightly greater distance of this borehole from the boundary with the Zatwarnica Member and the ambiguous dip of the layers, it can be inferred that thick-bedded Otryt sandstones dominate to a considerable depth in this borehole (to at last to 500 m below the surface), while the lower part of the profile cuts through the thin-bedded sandstone and shales of the Zatwarnica Member (Fig. 2B).

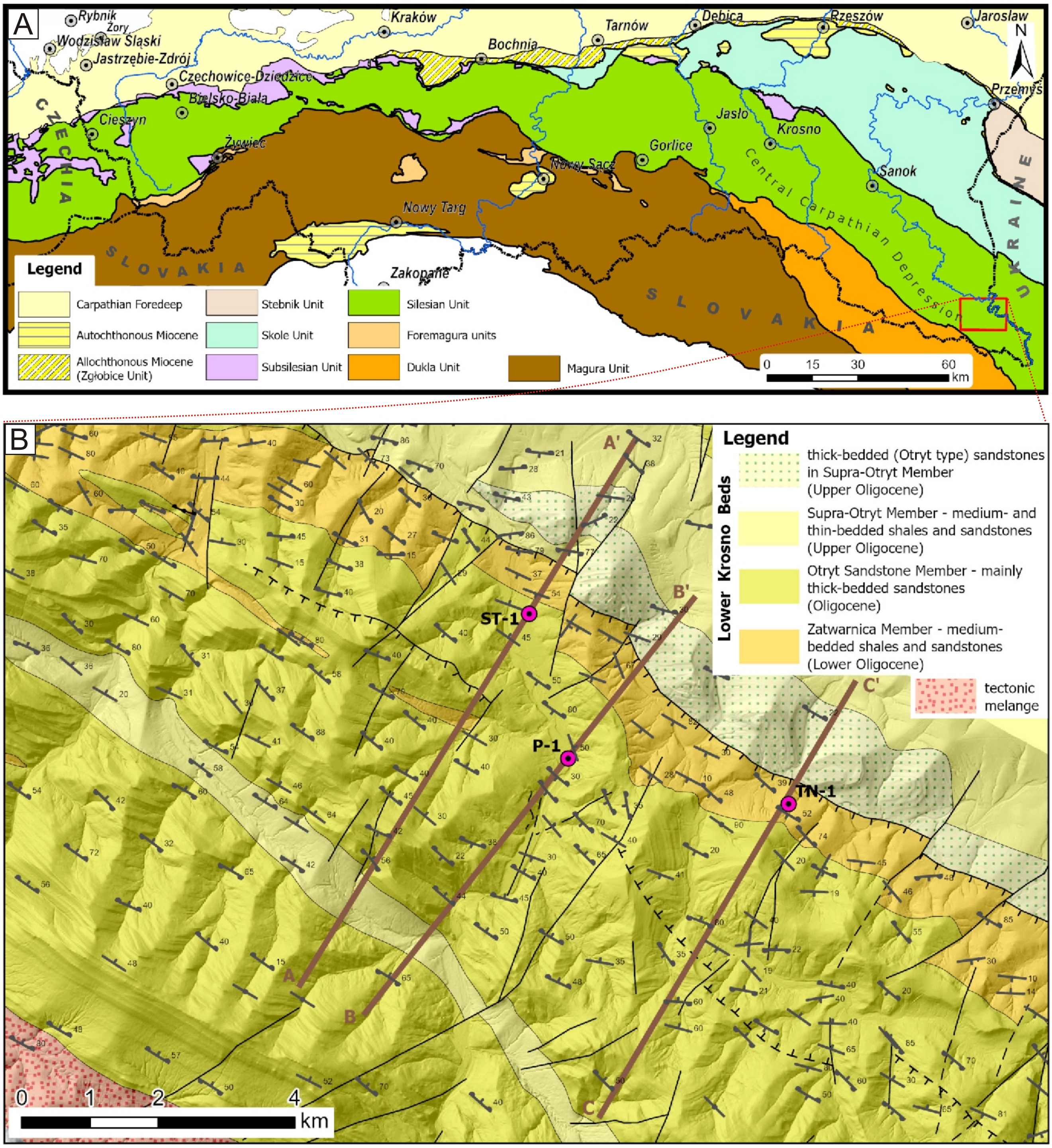

Fig. 1A – location of the study area (red rectangular) on a geological sketch of the Polish Outer Carpathians (based on Żytko et al., 1989, modified from Starzec et al., 2015); B – geological map of the study area with the location of the ST-1, P-1 and TN-1 boreholes

The lines AA', BB' and CC' on the map indicate the course of the geological cross-sections shown in Figure 2 (map based on Haczewski et al., 1998, 2001; Jankowski et al., 2004; Malata et al., 2006 and modified according to K. Starzec field investigations)

Table 1

Characteristics of lithostratigraphic units in the study area (age and thickness data based on Malata et al., 2014; Haczewski et al., 2016a, b)

	Menilite Beds	Transitional Beds	Lower Krosno Beds		
			Zatwarnica Member	Otryt Sandstone Member	Supra-Otryt Member
Lithology	brown, grey-black, bituminous shales and cherts with thin and medium-thick layers of greyish fine-grained sandstones (Krosno type)	coarse and medium-grained sandstones of the lower Krosno sandstone type, interbedded with brown and grey shales	dark grey, marly shales and mainly thin to medium-bedded fine-grained sandstones, subordinately thick-bedded sandstones	coarse-grained sandstones, grey, hard, with a large amount of muscovite,	grey, marly shales interbedded with thin to medium-bedded, fine-grained, calcareous sandstones
Age	Lower Oligocene	Lower Oligocene	Lower Oligocene	Oligocene	Upper Oligocene
Thickness	150–430 m	~200–300 m	~300–400 m up to 1200 m	From ~250 m in NW part to 1800 m in SE part	~1100 m

– the TN-1 borehole is located on the Zatwarnica Member that forms the frontal zone of the thrust fold (Fig. 2C). The Member is dominated by marly shales with interbeds of fine-grained sandstones. It can be concluded that at a relatively shallow beneath these layers (~400 m below the surface) there is a shale-sandstone succession forming the youngest member of the Krosno Beds in this area, i.e., Supra-Otryt Member comprising thin and medium-beded shales and sandstones; they form the southern limb of the next, more northern fold.

The Krosno Beds occur along almost the entire length of the stratigraphic columns used in the work described. The purpose of drilling of the P-1, ST-1, and TN-1 boreholes by the Polish Oil and Gas Company was to investigate the geological structure and lithofacies development of the Krosno Beds in the eastern part of the Zatwarnica thrust fold, as well as the structural conditions affecting the occurrence of hydrocarbon fields (Plezia, 1991a, b, c).

The geological and petrophysical information contained in the borehole report of these boreholes is consistent with the properties of the lithostratigraphical units as mapped regionally.

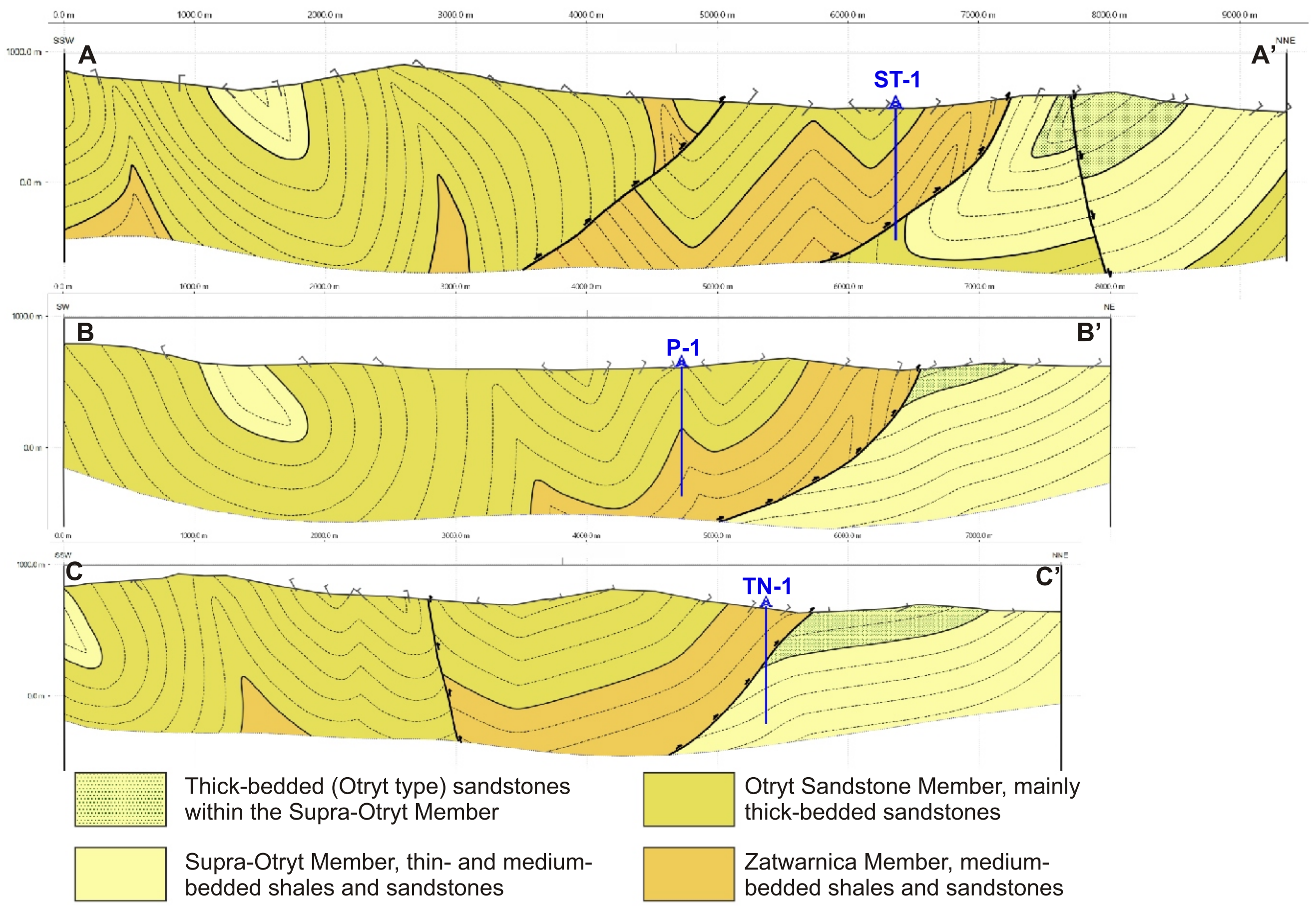

Fig. 2. Geological cross-sections along the lines shown in Figure 1B

MOVE software by PE Limited (Petex) was used in preparing the cross-sections

Table 2

Lithostratigraphic profiles of P-1, ST-1, TN-1 boreholes according to the borehole reports

Borehole	Top [m]	Bottom [m]	Stratigraphy and lithology description	Source/borehole reports
ST-1	0	10	Quaternary, gravel, sand and clays	Plezia (1991b)
	10	1014	Oligocene, Lower Krosno Beds, fine-grained sandstones with shale intercalations	
P-1	0	10	Quaternary, gravel, sand and clays	Plezia (1991a)
	10	1010	Krosno Beds, fine-grained, hard, strongly laminated with shale, traces of oil	
TN-1	0	900	Oligocene, Krosno Beds: weak-to-medium-grained shales, slightly sandy, fine-grained and micaceous sandstones, compact and wavy-banded	Plezia (1991c)

Table 2 summarizes the lithostratigraphic profiles of the P-1, ST-1, and TN-1 boreholes. The borehole reports does not include the division of the Krosno Beds into different members, differing in the ratio of sandstones to shales, because this distinction is difficult to make based solely on the examination of cutting samples. In this case, the interpretation of well logging data is important for the lithological and facies-based classification of the profile drilled through the Krosno Beds.

MATERIALS AND METHODS

The research material in the form of well logging data as well as descriptions of cores and cuttings contained in the borehole reports was provided by the Polish Oil and Gas Company (POGC, Warsaw, Poland) as part of the INGA INNKARP project no. POIR.04.01.01-00-0006/18-00 (2019–2023) financed in the frame of the Smart Growth Operational Program by the National Center for Research and Development and POGC, Warsaw, Poland.

The use of the INPEFA algorithm (PanTerra Geoconsultants, 2024) to identify facies and correlate deposits in the Krosno Beds of the Silesian Unit for better identification of reservoir zones was an innovative element in the study. For comparison, petrophysical facies were determined based on mineral composition (volume of shales VCL, and sandstones VSAND) from well logs, and facies determined by a geologist based on macroscopic descriptions of the cores and cuttings, as well as on geological observations in the field. The Rock Typing procedure was also incorporated, based on the determination of the Flow Zone Index (FZI), which defines the ability of rock to transmit reservoir fluids.

INPEFA ANALYSES

The use of the Cyclolog approach is based on the assumption that well logs reflect sedimentation conditions. Logging curves are a continuous record of lithofacies changes, and the geological information contained in the profiles can be mathematically described as a wave process (Nio et al., 1990, 2005). Continuous and evenly sampled records of well logs as a function of depth make them suitable for spectral analysis. Interruptions in the continuity of the sedimentation process, periods of erosion, or distinct changes in the type of rock material deposited in the sedimentary reservoir can be treated as phase changes in the wave record. In sandstone-shale rock sequences, such as those found in the rock formations of the Outer Carpathians, a set of well logs is used in the qualitative interpretation process to determine lithological boundaries and prepare illustrations of lithological sequences with varying sandstone to shale ratios. For this purpose, gamma ray (GR) and spontaneous potential (SP) logs are primarily used (Galloway, 1989; Catuneanu, 2006; Shouket and Jarzyna, 2014). Other types of logs commonly available in boreholes, i.e. neutron, acoustic and density logs, also provide data on lithological and facies changes, including information on fluid content in the pore space.

Each geophysical log, as a wave record, is treated as a combination of several waves of different frequencies (periods). In this approach, each wave component is associated with a specific stage of the sedimentation and lithology formation process. These components are visible in the logs as anomalies with varying periods. Well logs, treated as the sum of components, can be broken down into individual components using Fourier transform or other wave analysis methods (Huang et al., 1998; Gawędzki et al., 2015). Cyclolog uses PEFA (Spectral Change Attribute Analysis, Prediction Error Filter Analysis) and INPEFA (Spectral Trend Attribute Analysis, Integrated Predictive Error Filter Analysis; Nio et al., 1990, 2005). Both spectral analyses are based on MESA (Maximum Entropy Spectral Analysis), which uses the maximum entropy method. MESA is an effective way to break down the well log into components related to specific geological (sedimentary facies) conditions. It uses variable-length windows appropriate to the problem being solved by the interpreter. It shows the boundaries of lithological and facies changes that reflect changes in sedimentation conditions. PEFA (Prediction Error Filter Analysis) is a visualization of changes in the wave image. The maximum entropy method is used as a tool to predict the next point of discontinuity on the well log curve based on data previously analysed in a given window. As a final result, PEFA provides an error curve whose extreme values (positive or negative) are indicators of changes in amplitude or frequency of anomalies on the logging curve, interpreted as locations / depths of lithofacies changes. The PEFA image shows intervals dominated by positive or negative values. These are the result of geological changes, e.g. a predominance of positive PEFA values may indicate the dominance of shales over sandstones, and conversely, a predominance of negative values may indicate the dominance of sandstones over shales, both reflecting sedimentation conditions. Integration PEFA in intervals of similar formation gives INPEFA (Spectral Trend Attribute Analysis – Integrated Predictive Error Filter Analysis). INPEFA curves show intervals of increasing INPEFA trend as a function of decreasing depth, where positive peaks dominate, and intervals of decreasing INPEFA trend as a function of decreasing depth, where negative peaks prevail, and turning points separating the two trends dominate. From a geological point of view, a negative INPEFA trend indicates a transition from more clayey to more sandy deposits. Such trends, combined with knowledge of the mode of sedimentation and the depositional system of the strata under study, can be linked to specific changes in the sedimentary basin, e.g., especially in the case of sediments deposited in a relatively shallow environment like a shelf that is prone to sea level changes. A negative trend in the lithological profile may reflect regression and sea level fall. A positive trend, associated with a transition from more sandy to more clayey deposits, can be linked to the increasing depth of the sedimentary reservoir.

In the literature, there are many studies using PEFA and INPEFA techniques to correlate well logs in order to track lithological changes (Soua, 2012; Yuan et al., 2018; Nainggolan and Winardhi, 2019). Soua (2012) used three tools: facies association, Integrated Predictive Error Filter Analysis (INPEFA) of spectral gamma-ray data, and chemostratigraphy, for sequence stratigraphic analysis of the organic-rich and siliceous Cenomanian-Turonian succession in Tunisia to demonstrate the limits of correlation. Yuan et al. (2018) utilized spectral analysis technology – Integrated Prediction Error Filter Analysis (INPEFA) to effectively overcome the difficulty in correlating hydrocarbon-bearing conglomerates showing rapid vertical and horizontal lithological variations. Nainggolan and Winardhi (2019) conducted INPEFA analysis as an alternative approach to improve well log correlation in a case of limited biostratigraphy data.

The turning points on INPEFA curves, separating intervals with stable trends, are important for correlation. The Positive Bounding Point (PBP) is the point / depth where the trend changes from negative to positive. The opposite is true for the Negative Bounding Point (NBP). Negative Bounding Points (NBP) signal the end of a zone of increasing clay content and the beginning of an increase in the sandstone content of the formation. PBP signals the end of the zone with significant sandstone content and a shift towards increasing shale content. In this study turning points refer to the transitions from sequences dominated by mudstones / claystone / shales to those dominated by sandstones. These are distinctive, clear turning points on the INPEFA trend curves in the stratigraphic column. Against these trends, less distinct turning points stand out, which can be linked to thinner intervals.

The INPEFA values for all curves are shown on a scale of 0–1, so the magnitude of the anomalies on the curves are normalized in individual boreholes. Only trends were taken into account in the analysis.

INPEFA trends can be interpreted over long time intervals, in which case PEFA filters are selected at large depth intervals and longer MESA windows. If detailed geological conditions are of interest, INPEFA trends are considered at shorter intervals with smaller windows. The main objective of INPEFA is to increase the accuracy of level correlation based on well logging using changes in the spectral properties of the logs, lithofacies development, and changes in geological conditions. In this study, INPEFA trends were used to corroborate lithological changes in the Krosno Beds section and to highlight intervals of good reservoir properties.

PETROPHYSICAL LITHOFACIES

In selected boreholes in the Silesian Unit, in the interval of the Krosno Beds, a reinterpretation of well logging data was performed using ULTRA software (Halliburton) and Techlog software (Schlumberger), assuming a sandstone-clay rock model with a carbonate component (Alberty and Hashmy, 1984; Slb, 2019). For most of the old boreholes in the eastern Polish Carpathians, only a limited number of logs are available. In the study area, measurements from the first half of the 1970s and earlier include only radiometric logs, spontaneous potential logs, and gradient and potential resistivity logs. However, in each of the boreholes, reinterpreted logs provided information on the lithology and enabled the location of possible hydrocarbon-saturated intervals and source formations with elevated TOC (Total Organic Carbon) contents (Stadtműller et al., 2022).

The reinterpretation of old well logs with modern software provided several advantages. First, it enabled comprehensive and consistent lithological and reservoir characterization, including the calculation of mineral volumes such as clay (VCL), sandstone (VSAND), and carbonates (VLIME), as well as key reservoir parameters such as effective porosity (PHI), permeability (K), Total Organic Carbon (TOC), water saturation (SW) and irreducible water saturation (SWI). Before reinterpretation, the logs were corrected for measurement environment, normalized, and subdivided into lithostratigraphic units, which allowed the interpreter to apply appropriate parameters, developed for individual stratigraphic units based on core data, and improved the reliability of the interpretation.

All parameters computed were calibrated with extensive Routine Core Analysis (RCAL) and Special Core Analysis (SCAL) laboratory measurements of porosity, permeability, calcimetry, and reservoir test results, and also X-Ray Diffraction Analysis (XRD), and Nuclear Magnetic Resonance (NMR) data (if available). Calibration ensured high confidence in the results and confirmed that proper processing workflows had been applied. The three boreholes described come from a large database of well logs and laboratory measurements in the Eastern Carpathians. The integration of large multi-well datasets strengthened the regional consistency of the interpretation.

Additionally, the reinterpretation introduced a lithotype classification – distinguishing mudstones, sandstones, and carbonates based on clay volume – which had not been done previously for these boreholes. Using the calculated porosity and permeability, the Flow Zone Index (FZI) was also determined to provide valuable insight into reservoir flow behaviour and fluid mobility. The TOC calculation allowed identification of the most prospective source rock intervals, further enhancing the overall reservoir and source rock evaluation.

The reinterpretation of well logging data resulted in measurements of volumetric content of lithological components, including clay content (shaliness), and effective porosity, water saturation, irreducible water content, weight content of TOC, and permeability. A lithological model was developed for each borehole individually, depending on the availability of well logging data and the results of XRD laboratory analyses.

The clay minerals percentage (VCL) in the rock volume was the basis for defining petrophysical lithofacies: i) sandstone facies – VCL<35%, ii) mudstone facies – 35%<VCL<65%, iii) claystone facies – VCL>65%. Both the sandstones and shales of the Krosno Beds are rich in carbonates, therefore a carbonate facies was also inferred when the volume of the carbonate component (VLIME) was greater than 30%.

LITHOFACIES FROM GEOLOGICAL DATA

Based on the descriptions of cores and cuttings contained in the borehole report and knowledge obtained from field studies regarding lithofacial variability of the Krosno Beds in surface exposures, five lithofacies were defined on the percentage of sandstone and shale components (Table 3 and Fig. 3, lithofacies S-Sh). Additionally, one lithofacies of black shales (Sb) was also distinguished, based on the presence of thin intercalations of black or dark brown shales in various facies. Such intercalations indicate the presence of menilite-type shales among the Krosno Beds.

Table 3

Description of the lithofacies determined in the Krosno Beds in the boreholes studied, based on the descriptions of cores and cuttings contained in the borehole reports

Lithofacies code	Lithofacies	Lithological characteristics	Proportion of sandstone and shale [%]
S	sandstone	Fine-grained, less frequently medium-grained, calcareous sandstones with organic matter, occasionally interbedded with thin shales/mudstones	>85
SSh	sandstone, with shale	Sandstones, fine-grained, less frequently medium-grained, calcareous, with organic matter, interbedded with thin layers of shale	60–80
ShS	shale and sandstone	Sandstones, fine-grained, less frequently medium-grained, calcareous, with organic matter, and grey shales/mudstones, calcareous, with muscovite (similar proportions of both lithologies)	45–60
ShShS	shale-sandstone	Grey, calcareous shales/mudstones with muscovite, with a minor amount of fine- and very fine-grained calcareous sandstones	15–45
Sh	shale	Grey, calcareous shales with muscovite	<15
S_b	black shale	Thin interbeds of black or dark brown shales in various facies (S-Sh)	<15

ROCK TYPING BASED ON FZI

The concept of Hydraulic Flow Units (HFUs) is used to assess the ability of rocks to transmit reservoir fluids. A HFU is a representative elementary volume of the total reservoir rock having internally consistent geological and petrophysical properties (Amaefule et al., 1993). The methods for determining HFUs are based on the use of specific characteristics of porous rocks, such as pore shape, pore throat size and arrangement, and capillary pressure, in accordance with the original Kozeny-Carman model (Kozeny, 1927; Carman, 1937) and the construction of coefficients such as the Flow Zone Index (Amaefule et al., 1993; Alvarez et al., 2025) and the Resistivity Zone Index (Shahat et al., 2021). Effective porosity, PHI (a network of connected pores enabling fluid flow in a reservoir), and irreducible water volume (SWI) as results of reinterpretation of well logging data, formed the basis for calculating permeability K (Zawisza, 1993). Effective porosity PHI and permeability K allowed for the calculation of the Flow Zone Index FZI as the qualitative and quantitative indicator of zones with fluid flow ability. The FZI can be calculated according to formula (1):

$$FZI \quad 0.03014 \frac{\sqrt{\frac{F}{K}}}{\frac{F}{1 \quad F}} \qquad [1]$$

where: K – permeability [mD], F – effective porosity [dec] from reinterpretation of well logs.

The HFU concept was developed by several authors and Shahat et al., (2021) in their article described several approaches based on hydraulic FZI and electric RZI (Resistivity Zone Index) paths. Finally, Shahat et al. (2021) presented the equation for calculating RZI according to formula (2):

$$\log RZI \quad \log R_t \quad \log \frac{F}{1 \quad F} \qquad [2]$$

where: R_t – true electrical resistivity of rock.

These authors decided that reinterpreted old well log data provided more credible values of PHI and K than R_t. The FZI parameter was the basis for dividing the Krosno Beds section into Rock Types, which determine reservoir properties (Krakowska-Madejska et al., 2024).

RESULTS

The interpretation procedure is described using data from the P-1 borehole as an example. In addition to the results from the P-1 borehole, the results from the ST-1 and TN-1 boreholes were included in the set of laboratory analyses.

The results of the reinterpretation of well logging data in borehole P-1 covered the interval 12–1000 m (available from all the well logs). The FZI coefficient was calculated based on the effective porosity PHI and absolute permeability K. Basic statistics for selected petrophysical parameters are shown in Table 4. The limit values, Min and Max (i.e. range of changeability), as well as the arithmetic and harmonic means illustrate the variability of the interpreted values. Results of the reinterpretation are also shown on the collective drawing, which is discussed later, after including the results of other methods of facies determination.

Well logs were taken at 0.25 m intervals. Interpretation was performed using the same depth step. In the depth section 12–1000 m there was a large collected data set, in which it was necessary to determine values that had no physical manifestation. Permeability values K were limited from below by a value of 0.0002 mD. Similarly, PHI values equal to zero were not included in the statistical calculations. The lowest carbonate volume was 0.0001%. Harmonic means, always lower than arithmetic means, for quantities such as permeability or total organic carbon content, indicate a large number of low values for these parameters. Harmonic means close to arithmetic means for parameters such as PHI, VSAND, VCL, and GR indicate a normal distribution of these values. Comparable arithmetic and harmonic means of FZI indicate a significant proportion of higher and lower values of this parameter in the set. The estimated TOC value confirms the isolation of thin interbeds of black or dark brown shales (Sb) in various facies (S-Sh; Table 3). Infor-

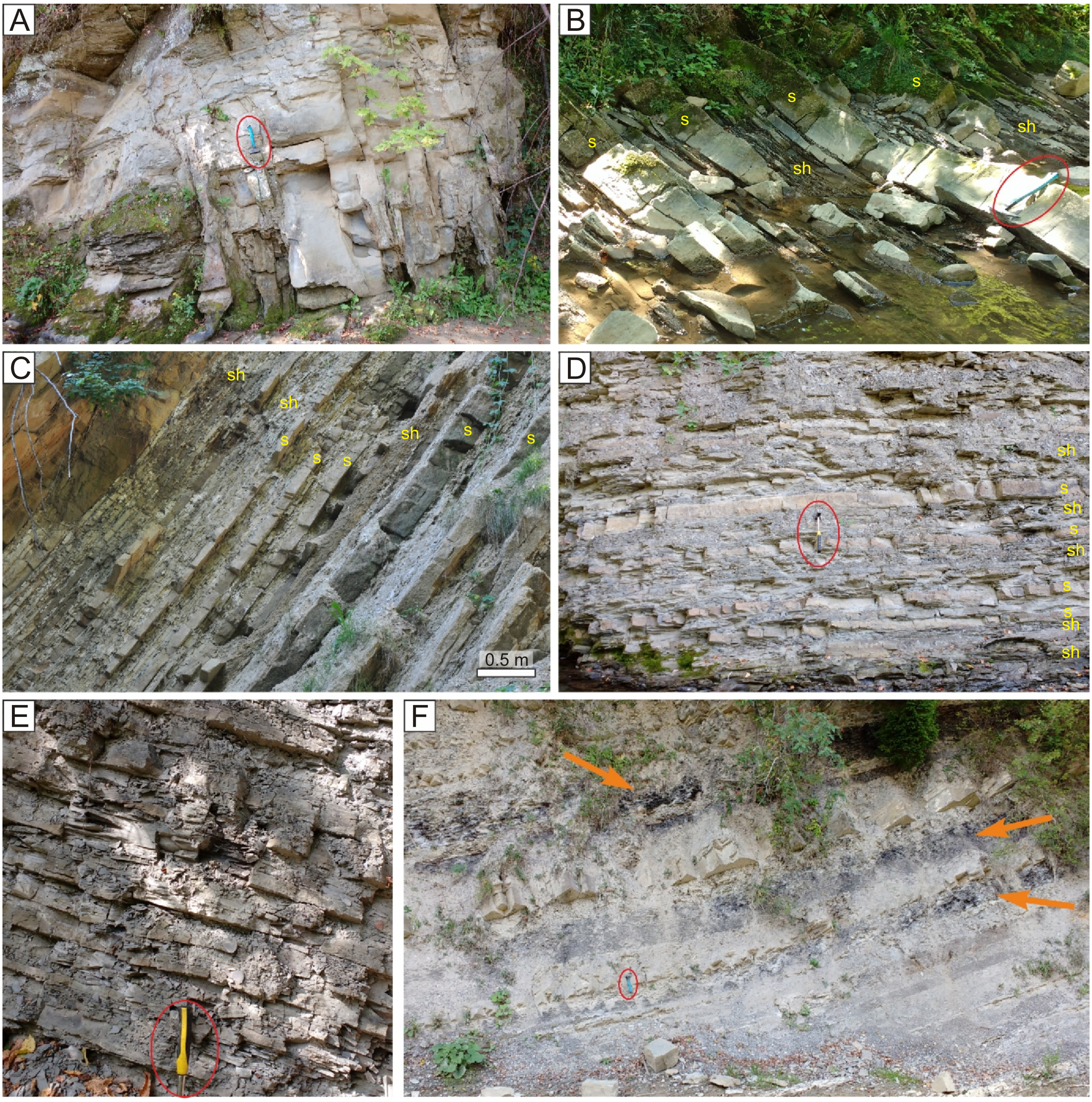

Fig. 3. Exposed examples of the determined lithofacies within successions of the Krosno Beds

A – very thick-bedded, massive or graded sandstones, occasionally interbedded with thin shales/mudstones – facies S (49°18'48.35"N, 22°22'16.63"Sh); **B** – facies SSSh dominated by thin- to thick-bedded sandstones, intercalated with thin shales (49°18'30.47"N, 22°16'34.83"E); **C** – package of thin- to medium-bedded sandstones and shales, facies SSh characterized by a similar proportion of both lithologies (49°38'9.91"N, 21°10'59.9"E); **D** – package of shales and very thin- and thin-bedded, find-grained sandstones – facies ShShS (49°11'1.05"N, 22°35'5.16"E); **E** – package of very thin-bedded shales/mudstones, rarely intercalated with thin layers of sandstone – facies Sh (49°12'47.2"N, 22°38'56.05"E); **F** – thin- to medium-bedded layers of black, bituminous shale of the Menilite type (facies S_b) – orange arrows, within grey shales and sandstones of the Krosno Beds type (49°12'9.01"N, 22°42'34.23"E). In the photos, some beds are labeled: sandstones with the letter "s" and shales with the letter "sh". Hammer marked with a red circle for scale, the coordinates of each exposure location are given in brackets

mation about black shales was included in the borehole report of borehole TN-1. Based on the results of the reinterpretation of well logs in the borehole discussed, the presence of three petrophysical lithofacies was identified: mudstone – over 60%; sandstone – over 30%; and carbonate – ~3%. Four FZI classes were defined based on FZI data from 3 boreholes being processed (P-1, ST-1, TN-1): i) FZI<0.5, ii) 0.5<FZI<1, iii) 1<FZI<2, iv) 2<FZI<4; and a histogram for P-1 borehole data was constructed according to those classes (Fig. 4). It was found that 52% of the data was in the class 1<FZI<2, and 32% in the class 2<FZI<4. The separate classes of FZI became the basis for Rock Types (RT). The same FZI classes were defined in the

Table 4

Basic statistics for selected petrophysical parameters, borehole P-1, depth interval 12–1000 m (Krosno Beds)

Parameter/ Statistics	PHI [%]	K [mD]	TOC [%w]	VCL [%]	VSAND [%]	VLIME [%]	SW [%]	GR [API]	RES [ohmm]	FZI [µm]
Min	0.04	0.0002	0.005	11	2	0.0001	43	41	18	0.22
Arithmetic Mean	5.75	1.518	0.819	38	36	20	95	72	37	1.66
Harmonic Mean	4.42	0.014	0.466	36	29	0.0175	94	69	34	1.29
Max	11.13	21.797	1.611	66	77	45	100	138	76	3.51

Symbols: PHI, VCL, VSAND, VLIME – results of comprehensive reinterpretation of the well logs, respectively: effective porosity, clay volume (shale content), sandstone and carbonate component volume, K and TOC – permeability and total organic carbon content values calculated on the basis of the reinterpretation results, GR – natural radioactivity, RES – electrical resistivity from measurements after environmental corrections, FZI – coefficient characterizing the rock's ability to enable fluid flow

three boreholes so that the RT values would be comparable. The sections of the geological profile characterized by high FZI values, calculated according to formula (1), correspond to rocks in which reservoir fluids flow easily. The relationship between FZI vs. porosity PHI and permeability K is non-linear; however, a combination of high PHI and K values indicates a high FZI.

Numerous traces of oil were observed during the drilling of borehole P-1, both in the mud as well as in cores. A flow of oil and gas was obtained from the perforated pipe at the depth interval 469–701 m (Plezia, 1991a). We expected changes in the basic statistics of the flow interval compared to the entire interval but Table 5 shows petrophysical parameter values very similar to those in Table 4.

The water saturation SW is similar in the entire interval and the flow interval, as is the volume of sandstone VSAND, while the shale content VCL is slightly lower in the productive interval. The reservoir parameters porosity, permeability, and FZI, as well as TOC, are similar in Tables 4 and 5. The percentage share of petrophysical lithofacies in the 461-701 m section changed in favour of sandstone (~37%; in the entire interval ~30%) at the expense of mudstone.

The FZI histogram was also calculated for the depth interval 461–701 m according to the previously selected classes (Fig. 5). The class 1<FZI<2 contained 56% of the data, while the classes 0.5<FZI<1 and 2<FZI<4 contained comparable amounts of data (~19% each). Currently, there is less data in the class FZI<0.5. The histograms in Figures 4 and 5 show the dominance of Rock Types (RT) in the class 1<FZI<2 for the entire profile and for the part with traces of oil. The larger amount of data in the 2<FZI<4 class in the entire set indicates that the layers with the best reservoir properties were not confined to the oil traces group. A slight effect of the presence of oil was also observed in terms of electrical resistivity. The RES values in Tables 4 and 5 are similar.

For the borehole P-1, as in boreholes ST-1 and TN-1, the facies classification was also prepared based on macroscopic core and cutting descriptions, and field geological information

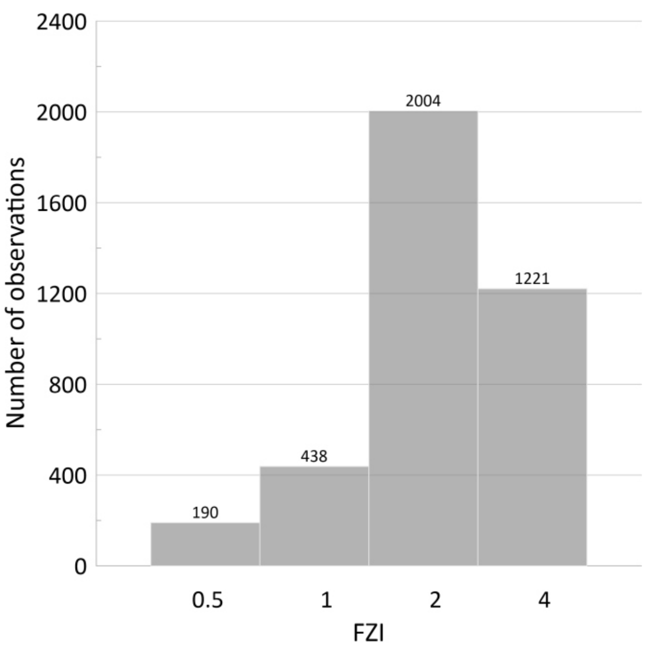

Fig. 4. FZI histogram, borehole P-1, depth interval 12–1000 m, Krosno Beds

Numbers at the top of the each bar show the number of data points in the class

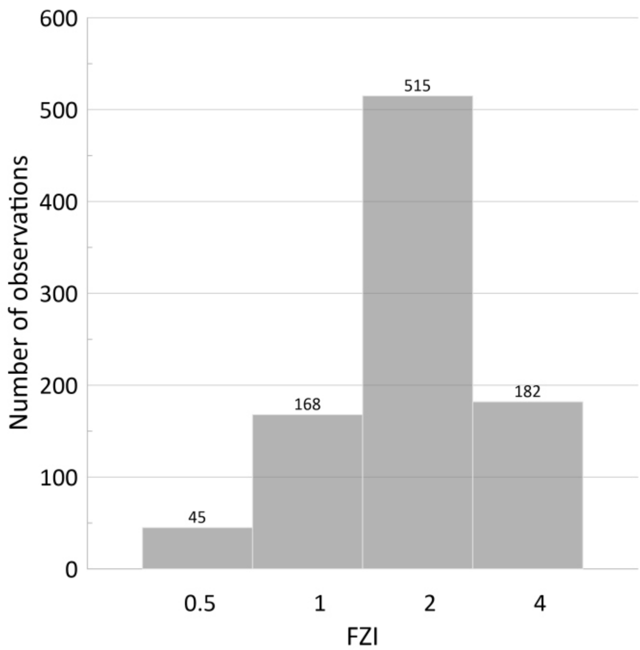

Fig. 5. FZI histogram, borehole P-1, depth interval 461–701 m, Krosno Beds

Numbers at the top of the each bar show the number of data points in the class

Table 5

Basic statistics for selected petrophysical parameters, borehole P-1, depth interval 469–701 m – oil flow (Krosno Beds)

Parameter/ Statistics	PHI [%]	K [mD]	TOC [%w]	VCL [%]	VSAND [%]	VLIME [%]	SW [%]	GR [API]	RES [ohmm]	FZI [μm]
Min	0.04	0.0002	0.023	14	8	0.0001	45	43	18	0.22
Arithmetic Mean	5.23	1.303	0.834	36	35	22	95	72	36	1.51
Harmonic Mean	3.41	0.012	0.562	34	29	0.0136	93	70	33	1.15
Max	11.13	21.797	1.611	59	77	45	100	131	67	3.51

Symbols as in Table 4

(Table 3). The lithofacies in these boreholes are similar in the individual profiles (Table 6) due to similar material (cores and cuttings) collected during drilling the same formations. The description of the facies contained in the borehole report confirms the similarity of the facies and lithology (Table 3). Table 6 revealed lithofacies that could be separated on the proportion of sandstone to shale (Table 3). Results are juxtaposed in Figure 6 to show the differences in vertical resolution of the methods shown.

Summaries of information on petrophysical facies, lithofacies, and Rock Types (FZI) in P-1 borehole are shown collectively in Figure 6. Interbedding of petrophysical lithofacies can be seen for mudstone and sandstone. The absence of petrophysical claystone facies (VCL>65%) indicates moderate shaliness of the formations studied, corroborated by the GR curve (Tables 4 and 5). The petrophysical carbonate lithofacies (VLIME>30%) at the 3% level shows that the profile is practically sandy-muddy throughout the entire interval. There is a clear correlation between higher Rock Types (orange) and sandstone facies, both as a result of well log reinterpretation (petrophysical lithofacies) and geological classification (lithofacies). High Rock Types are reflected in lithofacies S and SSSh, which are inherently sandstone-dominated. Lithofacies ShS (sandstone and shale) correlates with the mudstone petro-

Table 6

Classification into lithofacies of the Krosno Beds in boreholes P-1, ST-1, and TN-1 based on geological data contained in the borehole reports

P-1			ST-1				TN-1		
TOP [m]	BOTTOM [m]	FACIES	TOP [m]	BOTTOM [m]	FACIES	INFO	TOP [m]	BOTTOM [m]	FACIES
5	90	SSSh	10	40	SSSh		5	10	S
90	110	S	40	60	S		10	30	SSSh
110	160	SSSh	60	70	SSSh		30	50	S
160	180	ShS	70	90	S		50	60	SSSh
180	235	SSSh	90	100	ShShS		60	70	ShS
235	250	ShS	100	150	ShS		70	110	ShShS
250	275	SSSh	150	185	SSSh		110	120	ShS
275	285	S	185	240	ShS		120	150	ShShS
285	356	SSSh	240	255	SSSh		150	160	ShS
356	380	S	255	300	S		160	190	ShShS
380	390	SSSh	300	325	SSSh	S_b	190	200	ShS
390	405	S	325	335	S	S_b	200	280	SSSh
405	460	SSSh	335	365	SSSh	S_b	280	290	S
460	470	S	365	375	ShShS	S_b	290	310	SSSh
470	630	SSSh	375	380	ShS	S_b	310	385	S
630	660	ShS	380	430	ShShS	S_b	385	415	SSSh
660	670	SSSh	430	440	Sh	S_b	415	425	ShS
670	680	ShS	440	450	ShShS	S_b	425	455	ShShS
680	690	ShShS	450	500	SSSh	S_b	455	465	ShS
690	710	ShS	500	530	ShS	S_b	465	550	ShShS
710	720	SSSh	530	550	ShShS	S_b	550	570	ShS
720	735	ShS	550	580	ShS	S_b	570	590	SSSh
735	750	ShShS	580	635	SSSh	S_b	590	625	ShS
750	770	ShS	635	675	ShShS	S_b	625	660	ShShS
770	800	ShShS	675	685	ShS	S_b	660	740	ShS
800	850	ShS	685	730	ShShS	S_b	740	775	ShShS
850	920	ShShS	730	770	ShS	S_b	775	825	ShS
920	940	ShS	770	790	ShShS	S_b	825	880	ShShS
940	965	SSSh	790	825	ShS	S_b	880	900	ShS
965	980	ShS	825	870	ShShS	S_b			
980	990	ShShS	870	905	Sh	S_b			
990	1010	ShS	905	930	ShShS	S_b			
			930	940	Sh	S_b			
			940	960	ShShS	S_b			
			960	965	Sh	S_b			
			965	1010	ShShS	S_b			

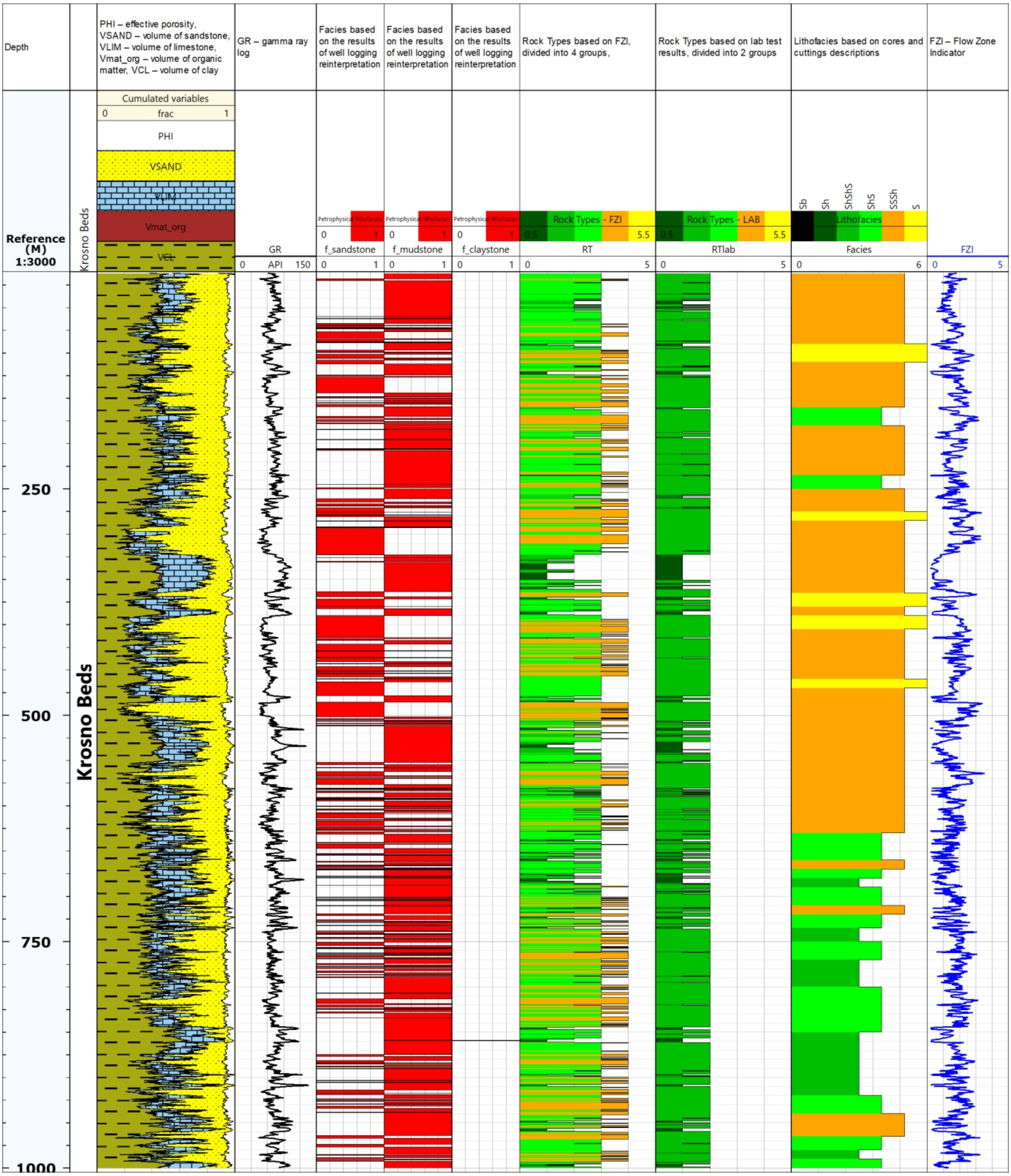

Fig. 6. Facies divisions in borehole P-1, depth interval 12–1000 m, Krosno Beds; scale 1:3000

physical lithofacies, which is clearly visible in the lower part of the profile. Lithofacies ShShS has also been identified in the lower part of the profile and generally correlates with the mudstone petrophysical facies. The sandstone petrophysical facies is observed in the form of thin interbeds. The Rock Types identified in the lower part of the profile occur in units of similar thickness to lithofacies ShShS. The small number of laboratory tests of porosity and permeability (11 pairs of porosity-permeability data) was the basis for the separation of only two Rock Types, RTlab, which did not specify the facies information (Fig. 6).

The facies divisions discussed above, based on petrophysical lithofacies and lithofacies determined on the basis of geological data and Rock Types, were supplemented with results from the Cyclolog algorithm. Studies using this program were performed on each borehole in the Krosno Beds interval using well logs, as GR, DT, SP and RHOB curves. The anomalies on the PEFA curves reflect lithological changes also visible on the logs (Fig. 7). The PEFA curves form the basis for calculating the INPEFA curves, which show the trends in the parameters measured by individual logs. Each INPEFA curve shows different details, although the general trends overlap (Figs. 7 and 8).

Figure 7 shows a part of the INPEFA graphs illustrating the results of analyses with different windows on the GR, DT and RHOB curves. The INPEFA curves show the variability of the rock; small and large changes can be analysed depending on the research goal. The selection of the window size, in which PEFA and INPEFA are calculated, is an important element of the analysis, depending on the objective. Moreover, it is possible to correlate changes in the GR and INPEFA curves. Natural radioactivity – gamma ray log GR, and the PEFA graph for the GR curve are shown on the left side of the INPEFA graphs.

The amount of detail visible in the graphs of results with windows of different width is similar. Trend change points are marked at almost the same depths. Trend change points also correlate with PEFA results, but are more pronounced. In detailed petrophysical analyses, results with a small window – 20 m – are more important. For structural analyses, results with a 40 m window are sufficient. It is clear that the INPEFA curves for windows of 40 m and above almost overlap. Cyclolog studies to compare lithofacies in all boreholes in the study were performed with the 40 m window. The size of the windows was dictated by the thickness of lithofacies (Table 6) and the vertical resolution of the well logs (~0.3–0.5 m).

The INPEFA curves are cumulative transforms of well logs that highlight geological discontinuities within the subsurface. These discontinuities in the log signal correspond directly to changes in geological conditions, and can therefore be interpreted as lithological changes or in special cases indirectly as changes in sedimentation rates. The INPEFA curve is the cumulative form; it converts pointwise discontinuities into broader upward or downward trends that can be interpreted stratigraphically. The INPEFA trend directions correlate with base-level and facies changes. Summarizing, positive trends (with INPEFA rising) correspond to transgressive phases, and indicate possible increasing shale content, deeper or quieter water. Negative trends (with INPEFA falling) are linked to regressive phases, indicating increasing sand content, and shallower or more energetic conditions in the marine environment. The INPEFA curves work as geological trend amplifiers, which take subtle variations in log data and convert them into cumulative curves that reveal the hidden structure of the sedimentary record. The positive and negative INPEFA trends in the sections of the Krosno Beds studied are similar across all boreholes and correlate similarly with the results of the other methods.

The P-1, ST-1, and TN-1 stratigraphic columns include INPEFA results based on GR, DT and SP logs, as well as reinterpretation results in the form of the clay content (shaliness) VCL, and effective porosity PHI. The GR and SP give the similar lithological answer, PHI and DT about the porosity, VCL and GR about the shaliness. There is a clear mutual correlation between the INPEFA trend curves. There is also a correlation between the anomalies on the gamma ray log and the trend curves. Such details cannot be observed on individual logs. Examples of logs and corresponding INPEFA trends from borehole P-1 are shown in Figure 8.

Based on the Cyclolog algorithm results recorded in the LAS format file, INPEFA graphs were constructed for borehole P-1, pairing graphs with similar information (Fig. 9), i.e. logs: GR and SP (lithology), and PHI and DT (porosity), and VCL and GR (shaliness)). INPEFA_SP gives additional anomalies compared to INPEFA_GR and INPEFA_VCL. The same applies to the INPEFA_DT and INPEFA_PHI curves. The different vertical resolution of the curves results in a variable image of the anomalies. The summary figure (Fig. 10) illustrates the facies distinguished by the different methods and the INPEFA curves in wells P-1, ST-1, and TN-1. The diverse information provided by different facies recognition techniques is clearly visible.

The best fluid flow properties (high FZI values) were observed in profile of the ST-1 borehole based on petrophysical lithofacies (FZI class: 5 and 4). Nevertheless, FZI class 4 reached a thickness of 785 m in the TN-1 borehole in comparison to the P-1 borehole – 305 m – and the ST-1 borehole – 157 m. Lithofacies determined on the basis of core descriptions and field samples showed the most sandy character for the profile in the P-1 borehole (S and SSSh lithofacies code), which reached ~628 m in thickness, while in the TN-1 borehole it reached 290 m and in the ST-1 borehole 345 m. Rock Types are consistent with lithological facies. Good media flow capacity is observed in the P-1 borehole, where sandstone and mudstone layers are interbedded and have similar proportions. The weakest flow capacity was observed in the ST-1 borehole. FZI class 1 reached ~171 m in thickness, while in the P-1 borehole it is ~72 m thick. There was no FZI class 1 in the TN-1 borehole. Numerous clayey intercalations are marked in this borehole on the lithofacies chart. The presence of thin interbeds of black shale in various facies (S-Sh; Table 6) may reduce the mobility of fluids. Their presence is also indicated by elevated TOC values. High RT values, very evenly distributed, and stable FZI values can be seen in the TN-1 borehole. The presence of shales (lithofacies ShShS) can be seen in all profiles.

The inclusion of INPEFA trend curves provided additional information. In the lower part of the profile in borehole P-1, where lithofacies ShS and ShShS are observed, a positive trend is marked for INPEFA_GR (red curve), INPEFA_SP (yellow) and INPEFA_VCL (green) associated with an increase in shaliness. Local changes in trends on the DT and PHI curves can be linked to the interlayers in lithofacies ShShS (the most clayey) and muddy lithofacies ShS.

In the case of borehole ST-1 (Fig. 10), INPEFA_GR (red curve) and INPEFA_VCL (green) follow a similar pattern. Additional details provided by the SP log are clearly visible. INPEFA_DT and INPEFA_PHI do not coincide. The trend graphs show an upward (positive trend) or downward (negative trend) trajectory, depending on the curve. The INPEFA_PHI (pink) and INPEFA_DT (blue) curves have a different course compared to the INPEFA_VCL and GR curves, and INPEFA_SP, which shows additional anomalies. A clear difference in the behaviour of the curves can be observed in the top interval, formed in the petrophysical lithofacies of sandstone, where INPEFA_DT and INPEFA_PHI run similarly but in opposite directions to INPEFA_GR and VCL.

The series of INPEFA curve analyses for the Krosno Beds is concluded by the TN-1 stratigraphic column (Fig. 10). The first clear change in the INPEFA_GR and INPEFA_PHI trend lines can be seen at a depth of ~420 m, where INPEFA_GR loses its negative trend and INPEFA_PHI loses its positive trend, the lithofacies ShS and ShShS indicating an increase in the proportion of shale to sandstone. A clear negative trend on the INPEFA_GR curve can be seen in the interval of lithofacies S and SSSh. This section also shows a more pronounced contribution from the petrophysical sandstone lithofacies. INPEFA_SP shows a negative trend, indicating an increase in sandiness from a depth of ~120 m.

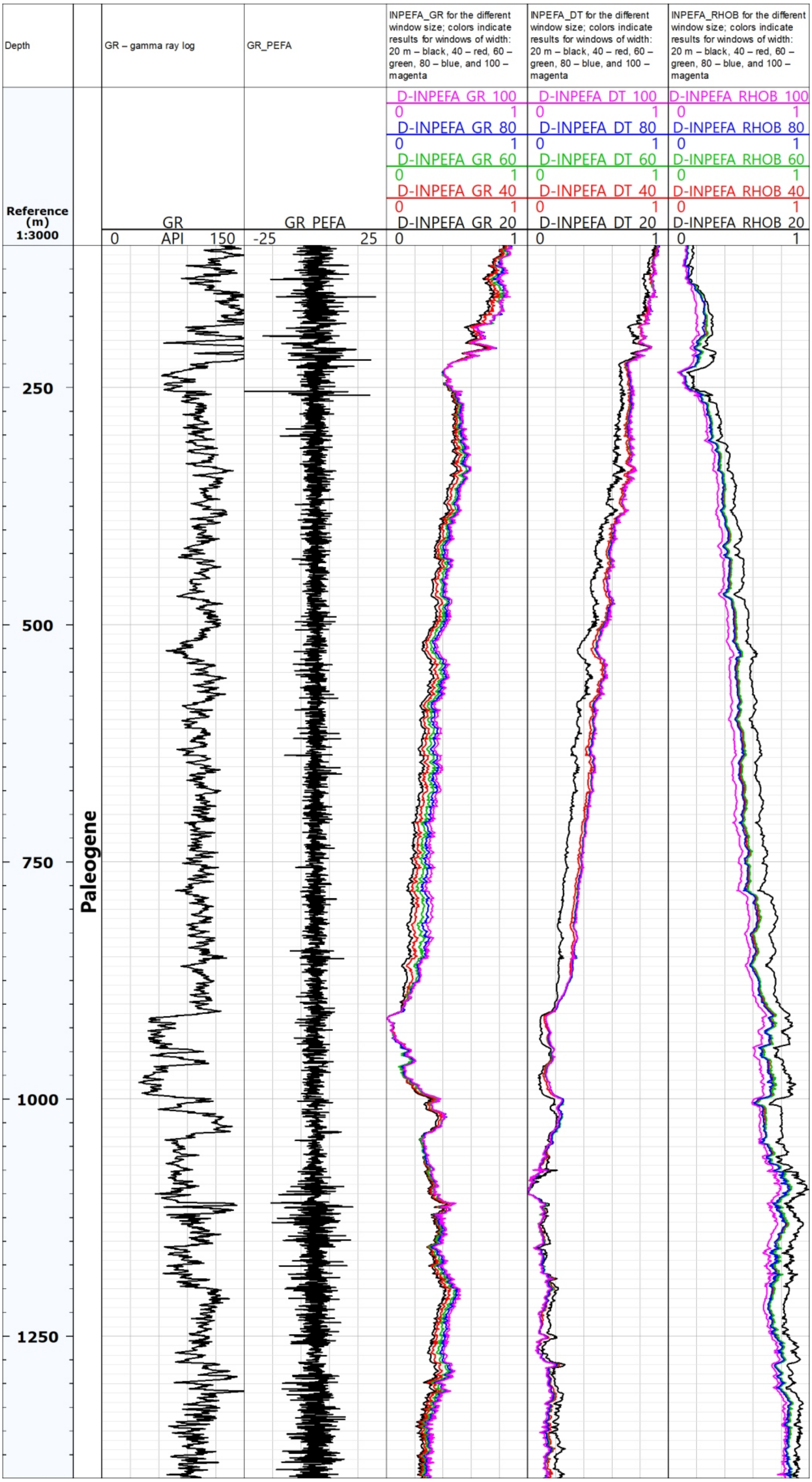

Fig. 7. Different window sizes for PEFA and INPEFA analyses

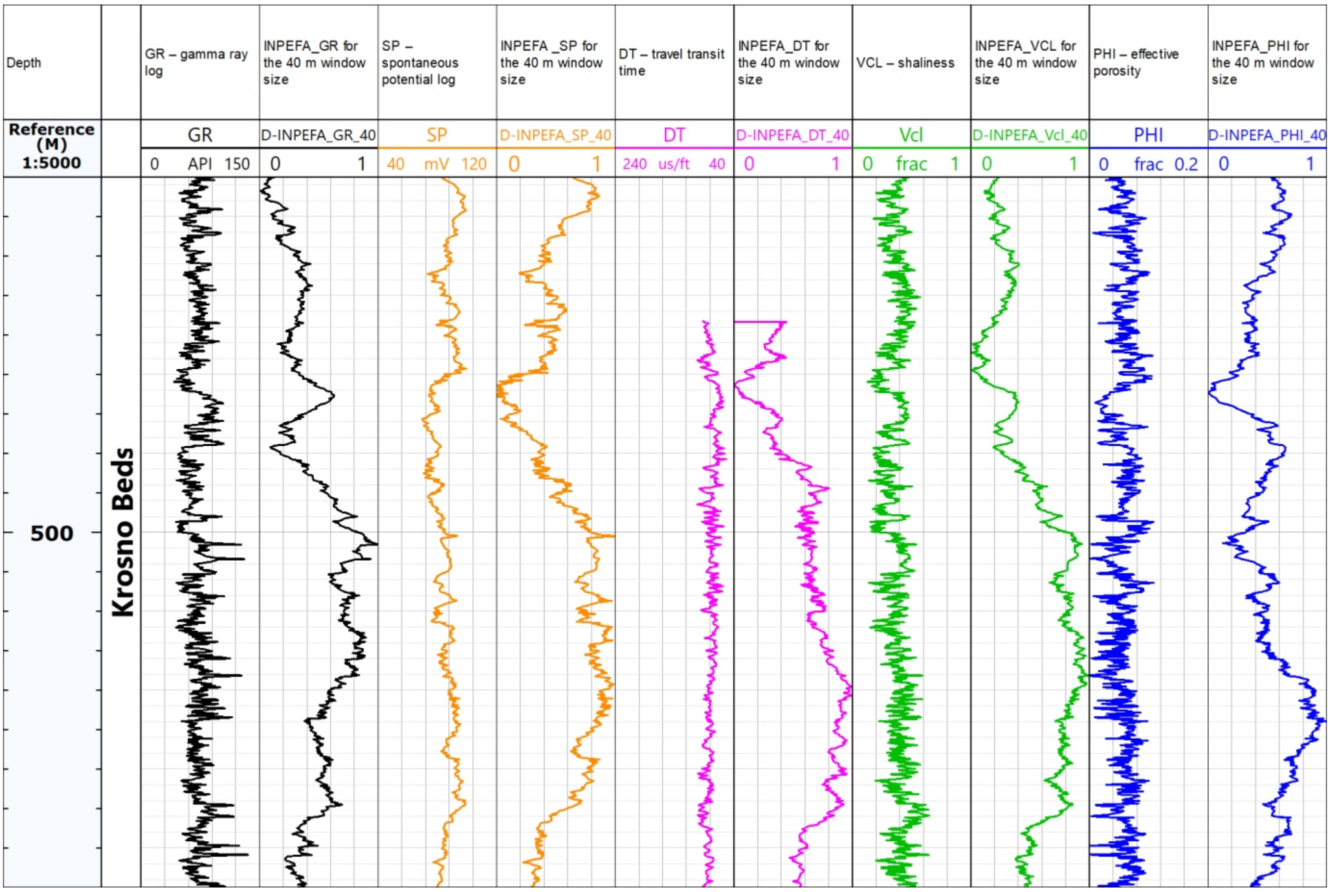

Fig. 8. INPEFA curves from Cyclolog in borehole P-1, Krosno Beds

DISCUSSION: CONTRIBUTIONS OF MULTI-SCALE AND MULTI-SOURCE INFORMATION TO LITHOFACIES IDENTIFICATION

All three boreholes, P-1, ST-1 and TN-1, show similar INPEFA_GR and INPEFA_VCL curves. The INPEFA_GR and INPEFA_PHI curves are reversed (as if they are mirror images), which is consistent with the physical interpretation of the effect of shaliness on porosity. The INPEFA_DT and INPEFA_PHI curves follow a similar trend in most intervals, but also show varying anomalies. The INPEFA_GR and INPEFA_SP curves look similar. The discrepancies in the GR and SP trend curves can be explained by the different physical basis of logs and different effects of shaliness in both curves. Nevertheless, the GR and SP curves are the basis for volume of clay (shaliness) calculations. The differences in the trends on the PHI and DT curves can be explained by the influence of saturation (borehole P-1) and possible changes in the composition of sandstone sections of the profiles (ST-1 – entire profile and TN-1 – lower part). The diversity of lithofacies determined on the base of macroscopic descriptions of cores, cuttings and field observations, as shown in Table 6, is also observed on the INPEFA curves in the form of local trend changes over short sections. On the INPEFA curve charts, the points of trend change do not always occur at the same depths, mainly due to the different vertical resolutions of the well logs, which affects the depth at which lithological boundaries are determined. From this perspective, FZI (Rock Types) and effective porosity analyses were carried out on the Krosno Beds studied (Table 7).

In borehole P-1, a detailed analysis was performed of the INPEFA_GR curves in the section 745.25–639 m and INPEFA_SP in the section 788.25–710.75 m, where in the case of the GR curve a clear upward trend is observed associated with a decrease in sand content, while the INPEFA_SP curve also maintains an upward trend, but the points of change in the trend on both curves are shifted in depth. A similar analysis was performed on the 845–745 m interval, where the INPEFA_GR curve shows a definite downward trend, while the trend on the INPEFA_SP curve is not uniform in this interval. In addition, the trend curves in the 882–845 m interval were analysed in detail, where both curves (INPEFA_GR and INPEFA_SP) show the same upward trend. In the interval 710.75–394.25 m on the INPEFA_DT and INPEFA_PHI curves, anomalies differ from those on the INPEFA_GR and INPEFA_SP curves. Two sections have been identified on the INPEFA_PHI curve: 515–394.25 m (upward trend, opposite to INPEFA_GR) and 701.75–515 m (downward trend). The section 701.75–394.25 m covers the depth interval from which the oil inflow was observed. A comparison of the average FZI and PHI values in Tables 4 and 5 did not show any significant differences. However, the results in Table 7 show a clear increase in FZI and PHI in the top part of this section.

Moreover, evaluated RT values (reflected by high FZI and PHI) are observed in intervals dominated by lithofacies ShS and ShShS. This behaviour may be related either to the vertical resolution of well logs or to the combined petrophysical response of lithofacies ShS and ShShS. The well log measurements were recorded at 0.25 m intervals; therefore, in the presence of thin

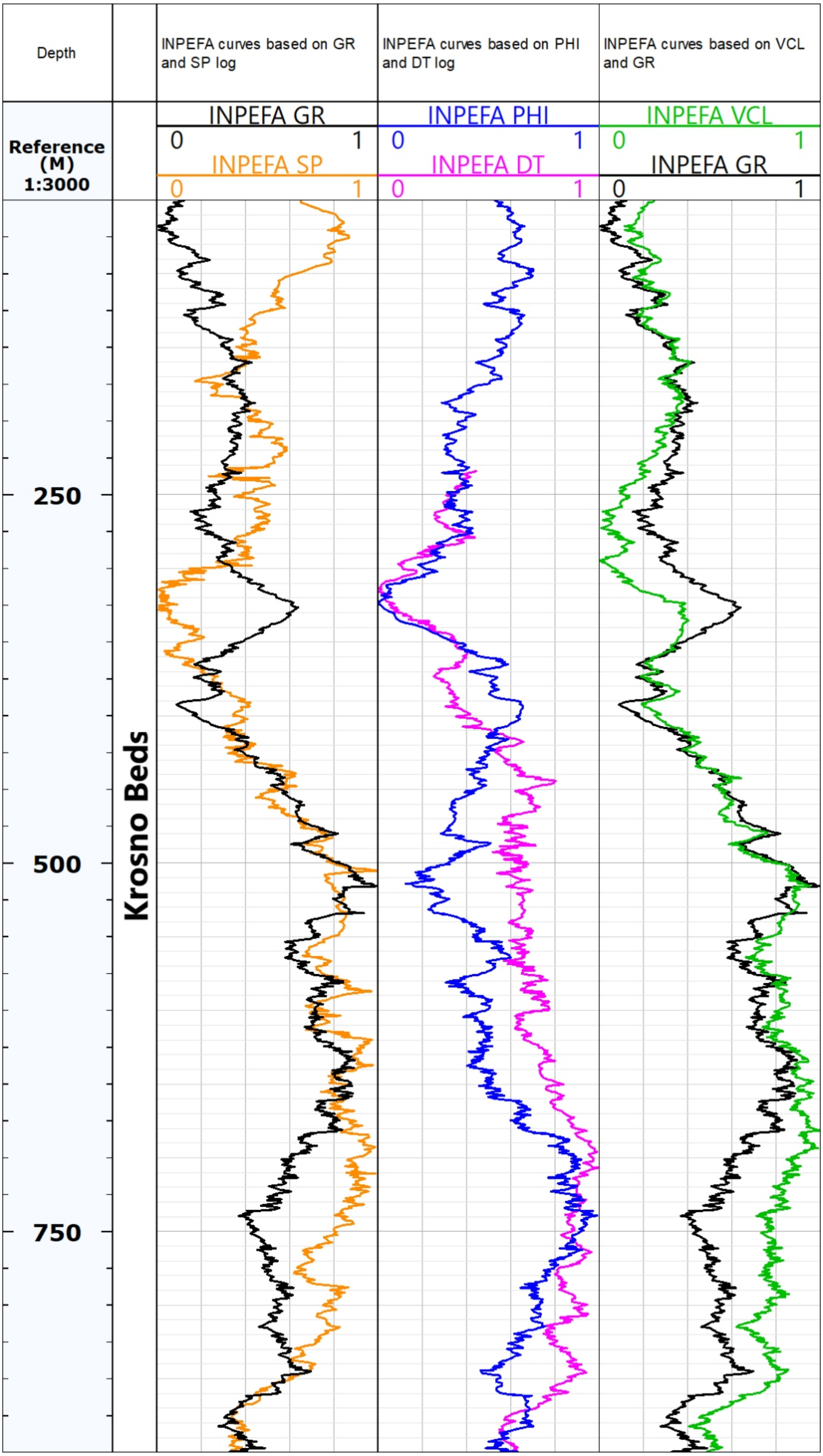

Fig. 9. INPEFA curves based on GR (black), SP (orange), DT logs (magenta), and VCL (green), and PHI (blue) interpretation results; borehole P-1; Krosno Beds

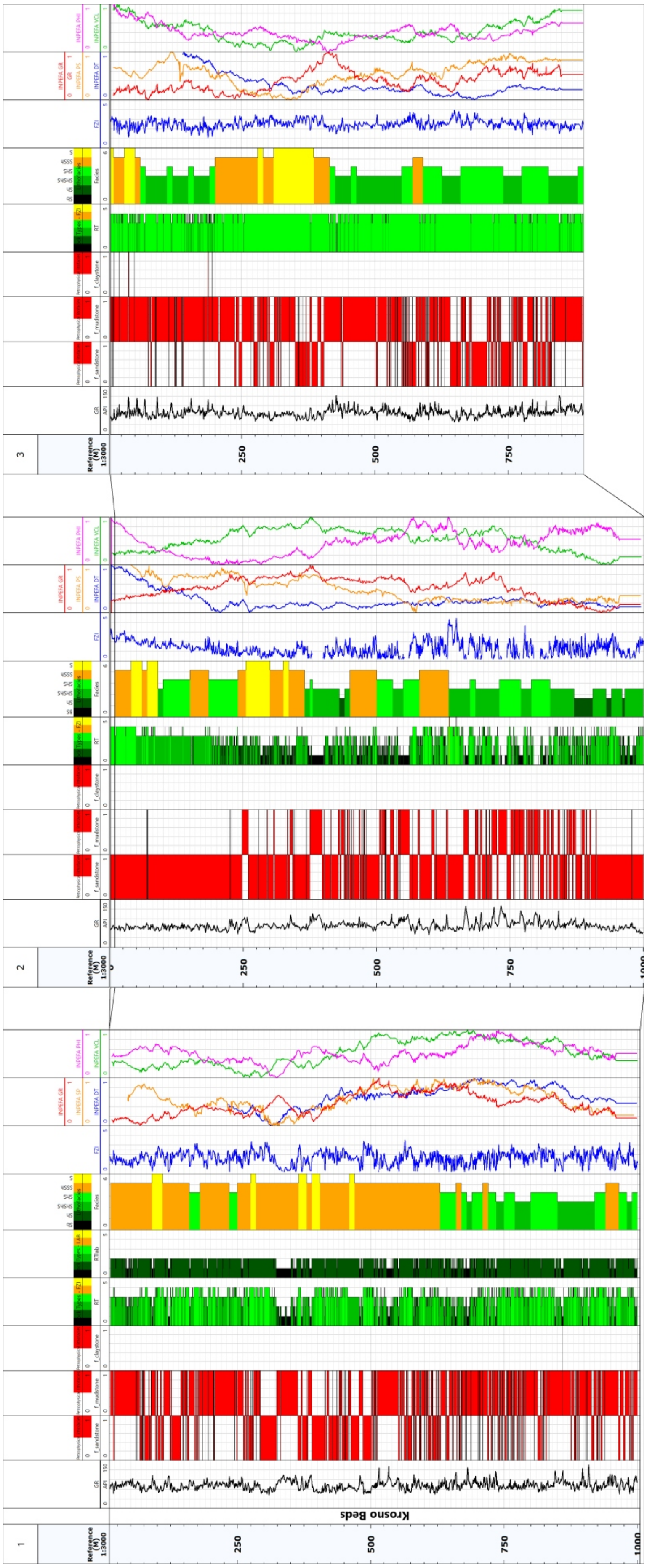

Fig. 10. Comparison of facies determined by various methods with INPEFA curves (GR – red, SP – orange, DT – blue, PHI – pink, VCL – green) in three boreholes marked as 1 – P-1, 2 – ST-1 and 3 – TN-1; Krosno Beds

Table 7

Changes in the trend on the INPEFA_GR curves and average FZI and PHI values in selected intervals in boreholes P-1, ST-1 and TN-1

Well	Depth interval [m]	Trend on INPEFA_GR curve	Log	Points of changes in trend	FZI [μm]	PHI [%]
P-1	272–193	upward	GR	PBP - NBP	1.63	5.76
	515–394.25	upward	PHI	PBP - NBP	1.91	6.49
	745.25–639	upward	GR	PBP - NBP	1.39	4.83
	788.25–710.75	upward	SP	PBP - NBP	1.82	6.16
	845–745	downword	GR	NBP-PBP	1.95	6.67
	882–845	upward	GR	PBP - NBP	1.54	5.19
	701.75–515	downword	PHI	NBP - PBP	1.42	4.97
ST-1	699–344	fluctuating	GR		1.28	4.30
	699–568	upward, fluctuating	PHI		1.82	5.90
	538–404	downword	PHI		0.95	3.72
TN-1	411–245	downword	GR	NBP - PBP	2.58	4.2
	550–411	upward, fluctuating	GR	PBP - NBP	2.40	3.6

layers, the log response is subject to vertical averaging. An alternative explanation for the pattern observed is the generally more favourable petrophysical properties of lithofacies ShS and ShShS, expressed by a combination of higher porosity and enhanced fluid flow capacity, which are locally less developed in lithofacies S.

The ST-1 borehole report contains information about oil flow during drilling from the 699–344 m interval. As in the P-1 borehole (Tables 4 and 5), the basic petrophysical parameter statistics for this section did not differ significantly from the statistics for the entire profile. This section was subjected to detailed examination, taking into account the variable trends on the INPEFA_PHI curve. The INPEFA_SP curve in this interval shows a generally upward trend, while the INPEFA_GR curve can be divided into two parts: the lower part with a downward trend and the upper part with an upward trend (more fluctuating). The interval 699–568 m shows elevated PHI value, compared to the entire interval studied (699–344 m) and the upper interval 538–404 m; the latter one is also characterized by significantly lower porosity (Table 7). It can be seen that both intervals differ significantly in terms of the parameters shown. The water saturation SW, was also calculated, which was 95% in the 699–304 m interval, 87% in the 699–568 m interval, and 99% in the 538–404 m interval. Changes in the INFERA_PHI trend prompted the calculation of water saturation (SW) in individual intervals in order to document the presence of oil traces. This example shows that it is worth analysing INPEFA trends from the PHI log.

In borehole TN-1, a detailed analysis of the INPEFA_GR curve was performed on the interval 550–245 m. A depth of 411 m divides the graph into two sections, the upper one showing a downward trend and the lower one showing an upward trend. The lithofacies correspond to the INPEFA_GR curve: the upper section is dominated by lithofacies S and SSSh, i.e., an increase in sandiness, while the lower section is dominated by lithofacies ShS and ShShS, i.e., an increase in shaliness. The average FZI values were calculated for both sections: 2.58 in the upper section and 2.40 in the lower section. The difference is not very large, both values classify RT in the highest class. RT determined at individual depth points does not show any significant changes. The average PHI in both intervals is 4.2% and 3.6%, respectively. The INPEFA_SP curve in the interval tested has a negative trend and shows several anomalies with smaller amplitudes, which can be interpreted as sandstones and mudstones with a large proportion of sandstone in the sandy-clay succession. The data in Table 7 and the graphs in Figure 10 show that sections with upward trends are generally associated with higher FZI values and higher (sandstone) RT classes, which is associated with higher porosity. The differences shown in the trend curves based on different logs allow for more detailed analyses of petrophysical parameters with a given MESA spectral study window. The study shows that adding INPEFA trends obtained from the Cyclolog program enriches petrophysical results and also translates into strictly geological information.

CONCLUSIONS

This study has demonstrated that INPEFA trend graphs based on spectral analysis of well logs are an effective tool supporting facies classification of the geological profile and helping to identify zones with better reservoir properties. The study described shows that information from various sources and on various scales, combined for a single purpose – lithofacies identification – results in a more accurate lithological recognition, which also affects reservoir properties. The trends obtained from the Cyclolog program made it possible to generalize very detailed and, by necessity, incomplete information from well logging and, at the same time, to responsibly incorporate independent, multi-scale data from cores, cutting samples, and field information.

The lithofacies determined in the sandstone-shale profiles of the Krosno Beds in three boreholes in the eastern part of the Outer Carpathians were examined on the basis of well logging and their quantitative interpretation, as well as lithofacies determined on the basis of geological knowledge obtained from field studies and macroscopic analyses of cores and cutting samples. INPEFA trends made it possible to generalize continuous information provided by petrophysical lithofacies and Rock Types in diverse lithologies. The study of INPEFA trend change points on various logs allowed for more accurate information and a more detailed examination of the causes of the anomalies observed in terms of lithological changes, porosity and saturation. The use of the spectral methods PEFA and INPEFA complements other standard geophysical techniques and core analysis. The results of the methods used complemented each other and confirmed the good reservoir properties of the most sandstone-rich parts of the profiles with decreasing INPEFA trends.

Acknowledgements. The results were obtained as part of the project entitled “Development of an innovative concept for searching for hydrocarbon fields in the deep structures of the Outer Carpathians”, INNKARP no. POIR.04.01.01-00-0006/18-00 (2019–2023), co-executed by AGH University of

Krakow, Poland, financed in the framework of the Smart Growth Operational Programme by the National Center for Research and Development and Polish Oil and Gas Company (POGC), Warsaw, Poland (Polish Oil and Gas Company (POGC) now Orlen SA). The authors would like to thank ORLEN SA, Warsaw, Poland for sharing their data and PAN Terra Geoconsultants for a paid lease of the CycloLog program for a specified period of time. Thanks are also extended to Dr. Monika Kasperska and Dr. Marek Stadtmüller for their contributions. The Techlog software was used thanks to Slb as a university program for AGH University of Krakow. This research was partially funded by the subsidy granted to the AGH University of Krakow by the Ministry of Science and Higher Education in Poland.

Author contributions: P.I.K.-M.: concept of research work and article structure, investigations, methodology, petrophysical interpretation, graphical side of the paper, edition; S.W.: concept and realization and interpretation of Cyclolog calculations, K.S.: field geological investigations, lithofacies definitions and descriptions, geological interpretation; E.P.: concept of research work, investigation, methodology, petrophysical interpretation; J.A.J.: concept of article, project administration, supervision, writing original draft; AL-Ś.: well logging interpretation, methodology.

REFERENCES

Alberty, M., Hashmy, K.H., 1984. Application of ULTRA to log analysis. SPWLA 25th Annual Logging Symposium, New Orleans, Louisiana, June 1984, SPWLA-1984-Z.

Alvarez, A., Missagia, R., Brito da Silva, R., Carrasquilla, A., 2025. Non-linear regression for permeability prediction and hydraulic flow units' characterization from core and well logs of a pre-salt carbonate reservoir in the Santos Basin, Brazil. Journal of Applied Geophysics, **241,** 105865; https://doi.org/10.1016/j.jappgeo.2025.105865

Amaefule, J.O., Altunbay, M., Tiab, D., Kersey, D.G., Keeland, D.K., 1993. Enhanced reservoir description: using core and log data to identify hydraulic (flow) units and predict permeability in uncored intervals/wells. SPE Annual Technical Conference and Exhibition, Houston, Texas, October 1993, SPE-26436-MS; https://doi.org/10.2118/26436-MS

Asquith, G., Krygowski, D., 2004. Basic Well Log Analysis (Second Edition) (with sections by Steven Henderson and Neil Hurley). AAPG Methods in Exploration Series, **16**.

Bała, M., Jarzyna, J., Mortimer, Z., 2012. Statistical analysis of petrophysical parameters of Middle Miocene rocks from the Polish Carpathian Foredeep. Geological Quarterly, **56** (4): 665–680; https://doi.org/10.7306/gq.1048

Carman, P.C., 1937. Fluid flow through granular beds. Transactions of the Institution of Chemical Engineers London, **15**: 150–156.

Catuneanu, O., 2006. Principles of Sequence Stratigraphy. Elsevier, Amsterdam, Boston, Heidelberg. Crain's Petrophysical Handbook, 2025; https://www.spec2000.net/index.htm (accessed 14 October 2025).

PanTerra Geoconsultants, B.V., 2022. Cyclolog® 2024.

Das, S., Singha, D.K., Mandal, P.P., Agrahari, S., 2024. Identification of lithofacies from well log data in the upper Assam basin using machine learning techniques. Acta Geophysica, **72:** 3191–3210; https://doi.org/10.1007/s11600-023-01229-8

Dziadzio, P., Ploch, I., Smoleń, J., 2021. Biostratigraphy and sequence stratigraphy of the Lower Cretaceous in the NW part of the Mid-Polish Trough. Geological Quarterly, **65,** 62; https://doi.org/10.7306/gq.1631

Galloway, W.E., 1989. Genetic stratigraphic sequences in basin analysis. I: Architecture and genesis of flooding-surface bounded depositional units. AAPG Bulletin, **73:** 125–142; https://doi.org/10.1306/703C9AF5-1707-11D7-8645000102C1865D

Gawędzki, W., Socha, M., Sławik, P., 2015. Decomposition of EEG signal in the time-domain using a Hilbert-Huang transformation HHT (in Polish with English summary). Przegląd Elektrotechniczny, **5:** 33–36; https://doi.org/10.15199/48.2015.05.09

Godlewski, P., Wendorff, M., Świąder, A., 2016. Compositional differences between Besko and Otryt sandstones of the Krosno Beds (Oligocene) in Eastern part of the Silesian Tectonic Unit. Geology, Geophysics & Environment, **42**: 73–74; https://doi.org/10.7494/geol.2016.42.1.73

Haczewski, G., Bąk, K., Kukulak, J., 1998. Detailed Geological Map of Poland 1:50 000 (in Polish), Dźwinacz Górny Sheet. Państwowy Instytut Geologiczny, Warszawa.

Haczewski, G., Bąk, K., Kukulak, J., Mastella, L., Rubinkiewicz, J., 2001. Detailed Geological Map of Poland 1:50 000 (in Polish), Ustrzyki Górne Sheet. Państwowy Instytut Geologiczny, Warszawa.

Haczewski, G., Bąk, K., Kukulak, J., 2016a. Explanations to the Detailed Geological Map of Poland 1:50 000 (in Polish), Dźwinacz Górny Sheet. Państwowy Instytut Geologiczny-PIB, Warszawa.

Haczewski, G., Bąk, K., Kukulak, J., Mastella, L., Rubinkiewicz, J., 2016b. Explanations to the Detailed Geological Map of Poland 1:50 000 (in Polish), Ustrzyki Górne Sheet. Państwowy Instytut Geologiczny-PIB, Warszawa.

Hallenburg, J.K., 1998. Standard Methods of Geophysical Formation Evaluation. Lewis Publishers. Boca Raton, Boston, London, New York, Washington, D.C.

Huang, N.E., Shen, Z., Long, S.R., Wu, M.C., Shih, H.H., Zheng, Q., Yen, N., Tung, C.C., Liu, H.H, 1998. The empirical mode decomposition and the Hilbert spectrum for nonlinear and non-stationary time series analysis. Proceedings of the Royal Society of London, A **454:** 903–995.

Jankowski, L., Kopciowski, R., Ryłko, W., 2004. Geological Map of the Outer Carpathians: Borderlands of Poland, Ukraine and Slovakia, 1:200 000. Polish Geological Imstitute, Warszawa.

Jankowski, L., Kopciowski, R., Ryłko, W., 2012. The state of knowledge of geological structures of the Outer Carpathians between Biała and Risca rivers – discussion (in Polish with English summary). Biuletyn Państwowego Instytutu Geologicznego, **449:** 203–216.

Kozeny, J., 1927. Über Kapillare Leitung des Wassers im Boden. Sitzungsber, **136** (2a): 271–306.

Krakowska-Madejska, P.I., Puskarczyk, E., Starzec, K., Jarzyna, J.A., Stadtmüller, M., 2024. Structure recognition and fluid flow potential based on well data and geological field investigations. A case study of the Istebna Beds, Silesian Unit, Carpathians. Geology, Geophysics & Environment, **50:** 357–381; https://doi.org/10.7494/geol.2024.50.4.357

Książkiewicz, M., 1977. The tectonics of the Carpathians. In: Geology of Poland. **4**, Tectonics (ed. W. Pożaryski): 476–620. Wydaw. Geol., Warszawa.

Ma, Y.Z., 2019. Facies and Lithofacies Classifications from Well Logs. In: Quantitative Geosciences: Data Analytics, Geostatistics, Reservoir Characterization and Modeling. Springer, Cham, **10:** 231–254; https://doi.org/10.1007/978-3-030-17860-4_10

Malata, T., Zimnal, Z., 2013. Explanations to the Detailed Geological Map of Poland 1:50 000 (in Polish), Sanok Sheet. Państwowy Instytut Geologiczny-PIB, Warszawa.

Malata, T., Jankowski, L., Żytko, K., 2006. Detailed Geological Map of Poland Polski 1:50 000 (in Polish), Lutowiska Sheet. Państwowy Instytut Geologiczny, Warszawa.

Malata, T., Jankowski, L., Żytko, K., 2014. Explanations to the Detailed Geological Map of Poland 1:50 000 (in Polish), Lutowiska Sheet. Państwowy Instytut Geologiczny-PIB, Warszawa.

Nainggolan, H.B., Winardhi, S., 2019. Geophysical approach to improve well correlation and stratigraphy package in the frontier area: example case of Upper Jurassic Fm. Semai Basin, Eastern Indonesia, IOP Conference Series: Earth and Environmental Science, **311,** 012054; https://doi.org/10.1088/1755-1315/311/1/012054

Nio, S.D., Bohm, A.R., Brouwer, J.H., De Jong, M.G.G., Smith, D.G., 1990. Climate Stratigraphy. Principles and Applications in Subsurface Correlations. EAGE Short Course Series; https://doi.org/10.3997/9789462820159

Nio, S.D., Brouwer, J., Smith, D.G., De Jong, M.G.G., Bohm, A.R., 2005. Spectral trend attribute analysis: applications in the stratigraphic analysis of wireline logs. First Break, **23:** 71–75.

Plezia, B., 1991a. Dokumentacja wynikowa odwiertu poszukiwawczego P-1 (in Polish). PGNiG S.A., Warszawa.

Plezia, B., 1991b. Dokumentacja wynikowa odwiertu poszukiwawczego ST-1 (in Polish). PGNiG S.A., Warszawa.

Plezia, B., 1991c. Dokumentacja wynikowa odwiertu poszukiwawczego TN-1(in Polish). PGNiG S.A., Warszawa.

Schlumberger, 1999. Log Interpretation Principles / Applications, 8th print. Sugar Land, Texas, Schlumberger Educational Services.

Serra, O., 2008. Well Logging Handbook. Editions TECHNIP, Paris, France.

Shahat, J.S., Balaha, M.I., El-Deab, M.S., Attia, A.M., 2021. Resistivity zone index: a new approach in rock typing to enhance reservoir characterization using well log data. Energy Reports, **7:** 711–723; https://doi.org/10.1016/j.egyr.2021.01.026

Shouket, A., Jarzyna, J.A., 2014. Reservoir properties and facies characterization from core data and well logging: autochthonous Miocene sediments in the Carpathian Foredeep case study. Geology, Geophysics & Environment, **40:** 331–342; https://doi.org/10.7494/geol.2014.40.4.331

Soua, M., 2012. Application of Facies Associations, Integrated Prediction Error Filter Analysis, and Chemostratigraphy to the Organic-Rich and Siliceous Cenomanian-Turonian Sequence, Bargou Area, Tunisia: Integrated Sequence Stratigraphic Analysis. Journal of Geological Research, **973195,** 15; https://doi.org/10.1155/2012/973195

Stadtmüller, M., Lis-Śledziona, A., Krakowska-Madejska, P.I., Jarzyna, J.A., 2022. Well logging and geological data for characterization of geological units, examples from the Silesian Unit, Polish Outer Carpathians (in Polish with English summary). In: Geopetrol 2022, Wyzwania dla sektora naftowego i gazowniczego w dobie transformacji energetycznej: Międzynarodowa Konferencja Naukowo-Techniczna, 19–21 September 2022, Zakopane, Oil and Gas Institute – National Research Institute, Kraków, 359–372.

Starzec, K., Malata, E., Wronka, A., Malina, L., 2015. Mélanges and broken formations at the boundary zone of the Magura and Silesian nappes (Gorlice area, Polish Outer Carpathians) – a result of sedimentary and tectonic processes. Geological Quarterly, **59**: 169–178; https://doi.org/10.7306/gq.1273

Ślączka, A., 1980. Explanations to the Geological Map of Poland 1:200 000, Łupków scheet (in Polish). Instytut Geologiczny, Warszawa.

Ślączka, A., Unrug, R., 1972. Regional and local variation of composition of the sandstones of the Krosno beds (Flysch Carpathians) estimated by variance analysis (in Polish with English summary). Rocznik Polskiego Towarzystwa Geologicznego, **42**: 373–395.

Slb, 2019. Techlog software manual.

Tiab, D., Djebbar, E.C., 2015. Petrophysics. 4th Edition. Gulf Professional Publishing.

Wang, Y., Wang, X., Wang, K., Fu, Y., 2025. Lithology recognition and porosity prediction from well logs based on Convolutional Neural Networks and sliding window. Journal of Applied Geophysics, **242,** 05905; https://doi.org/10.1016/j.jappgeo.2025.105905

Tołwiński, K., 1933. Centralna depresja karpacka (in Polish). Geologia i Statystyka Naftowa Polski, **11**: 362–366.

Wells, J.C., 1967. Geologic Interpretation from Well Logs. Standard Oil Company of California, San Francisco.

Wendorff, M., 1986. Facies relationship in the Krosno Beds in the eastern part of the Silesian tectonic unit: an outline of qualitative and quantitative analysis. In: 7th European Regional Meeting: Kraków – Poland, May 1986: excursion guidebook (ed. A.K. Teisseyre): 121–125. Ossolineum, Wrocław.

Yuan, R., Zhu, R., Qu, J., Wu, J., You, X., Sun, Y., Zhou, Y. N., 2018. Utilizing Integrated Prediction Error Filter Analysis (INPEFA) to divide base-level cycle of fan-deltas: A case study of the Triassic Baikouquan Formation in Mabei Slope Area, Mahu Depression, Junggar Basin, China. De Gruyter Open Access licensed under the Creative Commons Attribution Noncommercial-Noderivatives 4.0 License.

Zawisza, L., 1993. Simplified method of absolute permeability estimation of porous beds. Archives of Mining Sciences, **38:** 343–352.

Żytko, K., 1968. Geological structure of the Carpathians between the Strwiąż river and Wetlina in the Bieszczady Mountains (in Polish). Archiwum Geologiczne Oddziału Karpackiego PIG-PIB, Kraków.

Żytko, K., Gucik, S., Ryłko, W., Oszczypko, N., Zając, R., Garlicka, I., Nemčok, J., Eliáš, M., Dvořák, J., Stránik, Z., Rakus, O., Matějovska, O., 1989. Geological Map of the Western Outer Carpathians and their Foreland without Quaternary formations. Instytut Geologiczny, Warszawa.